



Contents lists available at ScienceDirect

Plant Science

journal homepage: [www.elsevier.com/locate/plantsci](http://www.elsevier.com/locate/plantsci)



# AIR12, a *b*-type cytochrome of the plasma membrane of *Arabidopsis thaliana* is a negative regulator of resistance against *Botrytis cinerea*

Alex Costa<sup>a,1</sup>, Raffaella Barbaro<sup>b,1</sup>, Francesca Sicilia<sup>c,1</sup>, Valeria Preger<sup>b</sup>,  
Anja Krieger-Liszkay<sup>d</sup>, Francesca Sparla<sup>b</sup>, Giulia De Lorenzo<sup>c,\*\*</sup>, Paolo Trost<sup>b,\*</sup>

<sup>a</sup> Dipartimento di Bioscienze, Università di Milano, Via G. Celoria 24, 20133 Milano, Italy

<sup>b</sup> Dipartimento di Farmacia e Biotecnologie (FABIT), Università di Bologna, Via Irnerio 42, 40126 Bologna, Italy

<sup>c</sup> Dipartimento di Biologia e Biotecnologia "C. Darwin," Istituto Pasteur-Fondazione Cenci Bolognietti, Sapienza Università di Roma, 00185 Roma, Italy

<sup>d</sup> Commissariat à l'Energie Atomique et aux énergies alternatives (CEA) Saclay, Institut de Biologie et Technologie de Saclay, Centre National de la Recherche Scientifique UMR 8221, 91191 Gif-sur-Yvette Cedex, France

## ARTICLE INFO

### Article history:

Received 12 August 2014

Received in revised form

27 December 2014

Accepted 3 January 2015

Available online xxx

### Keywords:

Plasma membrane redox

Cytochrome *b*

*Botrytis cinerea*

Apoplast

Ascorbate

Reactive oxygen species

## ABSTRACT

*AIR12* (Auxin Induced in Root culture) is a single gene of *Arabidopsis* that codes for a mono-heme cytochrome *b*. Recombinant *AIR12* from *Arabidopsis* accepted electrons from ascorbate or superoxide, and donated electrons to either monodehydroascorbate or oxygen. *AIR12* was found associated *in vivo* to the plasma membrane. Though linked to the membrane by a glycosylphosphatidylinositol anchor, *AIR12* is a hydrophilic and glycosylated protein predicted to be fully exposed to the apoplast. The expression pattern of *AIR12* in *Arabidopsis* is developmentally regulated and correlated to sites of controlled cell separation (e.g. micropilar endosperm during germination, epidermal cells surrounding the emerging lateral root) and cells around wounds. *Arabidopsis* (*Landsberg erecta*-0) mutants with altered levels of *AIR12* did not show any obvious phenotype. However, *AIR12*-overexpressing plants accumulated ROS (superoxide, hydrogen peroxide) and lipid peroxides in leaves, indicating that *AIR12* may alter the redox state of the apoplast under particular conditions. On the other hand, *AIR12*-knock out plants displayed a strongly decreased susceptibility to *Botrytis cinerea* infection, which in turn induced *AIR12* expression in susceptible wild type plants. Altogether, the results suggest that *AIR12* plays a role in the regulation of the apoplastic redox state and in the response to necrotrophic pathogens. Possible relationships between these functions are discussed.

© 2015 Published by Elsevier Ireland Ltd.

## 1. Introduction

The extracellular milieu of plants, known as the apoplast, includes cell walls, intercellular spaces and the lumen of xylem vessels, and is a living compartment where environmental cues are perceived and signals are generated to orchestrate adaptive responses [1]. The apoplast also includes an aqueous phase permeating primary cell walls, whose chemical composition can change depending on physiological and pathological conditions.

In the apoplast, reactive oxygen species (ROS) can be generated, both in physiological and pathological contexts [2–4], leading to an alteration of the redox state that has major effects on both cell wall organization and cellular responses to different types of stimuli [5].

Hydrogen peroxide, generated in the cell wall by the action of oxidases and peroxidases, is required for cross-linking reactions including lignin and suberin biosynthesis [1]. However, the same hydrogen peroxide required for strengthening the cell wall may also generate, under particular conditions, hydroxyl radicals, cell wall loosening agents implicated in auxin-induced cell wall elongation [6], fruit softening [7] and separation of the micropilar endosperm cells during germination [8].

On the other hand, the production of ROS is emerging as a key mechanism in the maintenance of cell wall integrity (CWI), a task entrusted to a surveillance system that modulates cellular functions by triggering signaling cascades. For example, the coordination of CWI and cell growth by THESEUS1 and FERONIA, two receptor-like kinases of the *Catharanthus roseus*

\* Corresponding author at: Laboratory of Plant Redox Biology, Department of Pharmacy and Biotechnology, University of Bologna, Via Irnerio 42, I-40126 Bologna, Italy. Tel.: +39 051 2091329; fax: +39 051 242576.

\*\* Corresponding author.

E-mail addresses: [giulia.delorenzo@uniroma1.it](mailto:giulia.delorenzo@uniroma1.it) (G. De Lorenzo),

[paolo.trost@unibo.it](mailto:paolo.trost@unibo.it) (P. Trost).

<sup>1</sup> These authors contributed equally to this work.

RLK1-like subfamily, involves ROS produced by NADPH-oxidases as downstream signals [9]. ROS and NADPH-oxidases play also a role in downstream signaling of oligogalacturonide (OGs), fragments of homogalacturonan that are *bona fide* signals for an altered CWI [10].

Besides plant development [11], cell wall remodeling and ROS are also deeply involved in plant–microbe interactions [3,4,12]. ROS are produced in all different levels of plant resistance to biotrophic pathogens [12,13] and play a complex role in interactions with necrotrophic pathogens. The necrotrophic pathogen *Sclerotinia sclerotium*, for instance, initially suppresses the oxidative reaction of the host Arabidopsis, but later it takes advantage from a second oxidative burst that triggers programmed cell death in the host tissue, thereby favoring pathogen proliferation [14]. *Botrytis cinerea*, which like *Sclerotinia* secretes oxalate to limit the initial oxidative burst, appears to behave similarly [15–17].

In the apoplast, ROS levels may be chemically controlled by low molecular weight antioxidants such as phenolics and ascorbate (Asc) [18,19]. By reacting with ROS, Asc is transiently oxidized to monodehydroascorbate radical (MDHA) that, in the apoplast, can be reduced back to Asc by plasma membrane (PM) cytochromes *b*<sub>561</sub> [20] or generate fully oxidized dehydroascorbate (DHA) by dismutation [21]. Uptake of DHA for cytosolic regeneration of Asc [22] and return to the apoplast, must compete with the rapid degradation of DHA in the apoplast [23]. As a result of all these concomitant activities, the redox state of the ascorbate pool in the apoplast is typically more oxidized and less buffered than in the cytosol, where the pool is much more concentrated and tend to be highly and steadily reduced [18,24]. Interestingly, export of Asc from the cytosol is stimulated by hydrogen peroxide [25] further supporting the ROS/Asc interplay in the apoplast [26].

AIR12 is one of the many redox proteins that may affect or be affected by the redox state of the apoplast. The gene *AIR12*, which exists as a single copy in the Arabidopsis genome, was originally described as an Auxin early-Induced gene of Arabidopsis Root cultures, in which lateral root formation was initiated by addition of the hormone [27]. Unexpectedly, ten years later, AIR12 was identified as an Asc-reducible cytochrome *b* [28]. This cytochrome was previously shown to be glycosylated [29] and associated to plasma membrane vesicles [30].

AIR12 is a hydrophilic protein predicted to be anchored to the plasma membrane by a GPI tail [28]. This prediction is confirmed by several proteomic studies [31–33]. Cytochromes *b*<sub>561</sub> (CYB561) form a different family of Asc-reducible cytochromes of plant cells, different from AIR12 for having a trans-membrane structure. Moreover, AIR12 binds a single heme, while CYB561s bind two [20,34]. AIR12 is made of a single domain called DOMON (dopamine monooxygenase N-terminal domain [35]). Interestingly, DOMON domains are often associated with other redox domains, like in plant CYBDOM proteins in which a DOMON similar to AIR12 is inserted on top of a CYB561 domain, possibly forming an intramolecular redox chain extending into the cell wall [20,36]. AIR12 was also found associated with lipid rafts [37,38], a property shared with other redox proteins [37], including CYBDOMs [37,39] and CYB561 [40]. However the physiological role of AIR12 *in vivo* is unknown, and a function connected to the apoplastic redox state can only be hypothesized.

Here we provide *in vivo* experimental evidence for the plasma membrane localization of AIR12, and show that Arabidopsis AIR12 is a cytochrome *b* that is reduced not only by Asc but also by superoxide, and oxidized by either MDHA or oxygen. Moreover, we show that plants overexpressing AIR12 contain higher basal levels of ROS and that AIR12 gene expression tends to be restricted to sites where controlled processes of cell separation occur (e.g. micropilar endosperm during germination, sites of lateral root emergence, floral organs abscission zones) and is also induced by wounding. Interestingly, Arabidopsis AIR12 plays a role in the interaction with

the necrotrophic pathogen *B. cinerea*: knock-out mutants are less susceptible to the fungus, which, in turn, induces the expression of *AIR12*. Altogether, the results suggest that AIR12 plays a role in the regulation of the apoplast redox state and in the response of the plant to abiotic and biotic stress.

## 2. Materials and methods

### 2.1. Chemicals

All chemicals were from Sigma–Aldrich (Milan, Italy) or Merck (Milan, Italy) unless otherwise stated.

### 2.2. Cloning, expression and purification of *Arabidopsis thaliana* AIR12

The full-length cDNA of *Arabidopsis thaliana* AIR12 (At3g07390) was directly amplified from genomic DNA, since the gene contains no introns. The cDNA was first subcloned into an appropriate commercial vector (p35S-2), utilizing the following pair of primers 5'-AAAGGATCCATGTCCTGTGTCTTAAATACC-3' (*Bam*HI site, underlined) and 5'-AATGAATTCGAGAGACTAGAGAGAGATCC-3' (*Eco*RI site, underlined). The mature and soluble form of AIR12 (sAIR12), truncated of both the N-terminal signal peptide and the C-terminal GPI-insertion sequence, was amplified by PCR with the following primers 5'-TAGCGGCCGACGACACCCCGGCGAAG-3' (*Not*I site, underlined) and 5'-TGAATTCAGGCTTGCAATCACAGAACTTG-3' (*Eco*RI site, underlined) and transferred in frame with the c-myc epitope and a polyhistidine tag into the expression vector pPICZαB (Invitrogen). *Pichia pastoris* X-33 cells (Invitrogen) were transformed with pPICZαB-sAIR12 and selected on YPDS medium containing 1.5 mg/mL Zeocin™. Positive clones were tested for integration by PCR screening.

Protein expression and purification were performed as described in Ref. [28]. Pure recombinant sAIR12 protein was analyzed on 12.5% acrylamide gels, before and after deglycosylation with endoglycosydase-H (New England BioLabs), performed according to the manufacturer's instructions. Glycoprotein staining was performed according to Ref. [41].

### 2.3. Molecular characterization of the recombinant protein (sAIR12)

Concentration-dependent ascorbate (Asc) titrations were performed in a quartz cuvette containing 2 μM sAIR12 in 50 mM MES (pH 5.5). Final Asc concentrations between 0.1 μM and 20 mM were obtained with 1 μl additions of stock solutions with different Asc concentrations. Absorbance values at 560 nm were normalized to the absorbance of the fully reduced protein obtained with dithionite, and interpolated by nonlinear regression with a sigmoidal equation:

$$\% \text{sAIR12 reduction} = \frac{100}{(1 + S_{0.5}/[\text{Asc}])}$$

in which  $S_{0.5}$  represents the Asc concentration giving half reduction of 2 μM sAIR12 at equilibrium.

Time-dependent sAIR12 reduction by 1 mM Asc was performed with 1 μM purified protein in 50 mM MES (pH 5.5). For reduction by superoxide, a solution of 1 μM of sAIR12 in 50 mM Tris–HCl, pH 7.0, 150 mM KCl, 1 mM xanthine, was monitored before and after addition of 0.2 units of xanthine oxidase. Time-dependent sAIR12 oxidation by monodehydroascorbate (MDHA) was recorded after addition of 1 unit of Asc oxidase to a solution of 1 μM sAIR12, 50 mM MES, pH 5.5, previously equilibrated with 0.6 mM Asc. For autoxidation experiments, a solution containing 1 μM sAIR12, 50 mM MES, pH 5.5, 0.6 mM Asc, was let equilibrate for 30 min. Then the

buffer was exchanged by gel filtration to an identical buffer with no Asc, and the redox state of sAIR12 spectrophotometrically detected. In all experiments the percent reduction of sAIR12 was calculated from reduced-minus-oxidized spectra of the  $\alpha$ -band. For normalization, 100% reduction was obtained by dithionite addition.

#### 2.4. Plants growth conditions

If not otherwise stated, *Arabidopsis thaliana* plants were grown on soil in a growth chamber at constant temperature of 22 °C, under 12/12 h light/dark cycle and photosynthetic photon flux density of 100  $\mu\text{mol m}^{-2} \text{s}^{-1}$ .

#### 2.5. Isolation of the homozygous knock out mutant (AIR12-ko)

A knock out mutant carrying an insertion (DS enhancer trap) in the single exon of AIR12 in the *Arabidopsis* ecotype Landsberg erecta (Ler-0) was obtained from the CSHL collection (ET8602). The presence of the insertion was confirmed by PCR-based genotyping and a homozygous line was selected (AIR12-ko). In order to perform the RT-PCR analysis, total RNA from 10-days-old plants (either Ler-0 or AIR12-ko) was extracted and the cDNA was synthesized from 1  $\mu\text{g}$  total RNA as previously described [42]. The PCR was performed using primers designed at the 5'- and 3'-end of the AIR12 coding sequence. The forward and reverse primers were as follows: 5'-AAACAAGCTTCATGTCCCTGTGTCTTAAATACC-3' and 5'-AATGAATTCGAGAGACTAGAGAGATCC-3'. As internal control of cDNA quality we used the GAPC-1 (At3g04120) with the following forward and reverse primers: 5'-GCAAAGACGCTCCAATGTTGTG-3' and 5'-GAAGCACCTTCCGACAGCCTTG-3'. The PCR reaction was performed by the GoTaq polymerase (Promega) with the following parameters: 30 s at 94 °C, 30 s at 58 °C and 60 s at 72 °C. The PCR reaction was stopped at 35 cycles for AIR12 and 25 cycles for GAPC-1.

#### 2.6. Generation of AIR12 complemented lines (AIR12-comp)

The complemented lines were obtained by the transformation of AIR12-ko mutant with a 2802 bp genomic fragment of AIR12. The selected genomic region included 1554 bp of the promoter region, 822 bp corresponding to the AIR12 coding sequence and 426 bp downstream the stop codon. The genomic sequence was PCR amplified using Advantage 2 Polymerase (BD, Clontech, [www.clontech.com](http://www.clontech.com)) using the same forward primer used for promoter amplification, in combination with the reverse primer 5'-CATGCTCGAGGCTAGAGAGTCTAATGTTGCCCTAATCA-3' where an XhoI restriction site (underlined) was introduced. The amplicon was digested with EcoRI and XhoI restriction enzymes and ligated into the pGreen0229 binary vector [43]. The obtained clone named pGreen0229-AIR12comp-genomic was introduced into the *Agrobacterium tumefaciens* GV3101 strain and the AIR12-ko line was transformed by floral dip method [44] and screened on half-strength MS agar medium containing 250  $\mu\text{M}$  of BASTA.

#### 2.7. Generation of GmAIR12 over-expressing lines (GmAIR12-oe)

The coding sequence of *Glycine max* AIR12 (Glyma03g22260; [28]) was splitted in two parts. The N-terminal part, coding for the predicted signal peptide (SP) [45], was fused upstream the YFP coding sequence in the pAVA554 vector [46] and then the C-terminal end, including the predicted GPI-anchoring sequence [47], was placed downstream the YFP. The construct was under control of the double 35S promoter and the nos terminator. The entire cassette 2  $\times$  35S-SP-YFP-GmAIR12-nos was subcloned in the pGreen0029 binary vector [43] and introduced in *Agrobacterium tumefaciens* GV3101 strain. Wild type *Arabidopsis* plants (Ler-0) were transformed by floral dip method [44] and screened on half-strength

MS agar medium containing 50  $\mu\text{g}/\text{mL}$  of kanamycin. Only two GmAIR12-overexpressing transgenic lines (GmAIR12-oe) were obtained and genotyped by PCR with the following pair of primers 5'-TCCGCCCTGAGCAAAGAC-3' and 5'-GACGGAGAGGGAGCGGT-3' on 500 ng genomic DNA. Segregation analysis was carried out by growing seed progeny of T2 transgenic plants on a half-strength MS solid medium containing kanamycin (50  $\mu\text{g}/\text{mL}$ ). All the experiments were conducted on single insertion homozygous T3 plants.

#### 2.8. RT-PCR analyses

Plants were grown at a constant temperature of 22 °C under 12 h light/12 h dark cycle and total RNA was extracted as described in Ref. [48]. Four plants were collected for each RNA extraction and three independent extractions were performed. RNA was treated with RQ1 DNase (Promega) and first-strand cDNA was synthesized using ImProm-II reverse transcriptase (Promega) according to the manufacturer's instructions.

Expression analysis of *Arabidopsis thaliana* AIR12 (AtAIR12) by RT-PCR was performed in wild type (Ler-0), AIR12-comp and GmAIR12-oe plants. The expression level of *Glycine max* AIR12 (GmAIR12) was analyzed on Ler-0 and GmAIR12-oe plants. RT-PCR was carried out on 50 ng of cDNA obtained from a pool of three independent cDNA preparations and GmAIR12 gene expression was normalized to UBQ5 used as housekeeping gene. Quantification was performed with ImageJ software and expressed in arbitrary units. Primers for analysis of GmAIR12, AtAIR12 and UBQ5 transcripts were the following: GmAIR12-Fw: TCCGCCCTGAGCAAAGAC; GmAIR12-Rev: GACGGAGAGGGAGCGGT; AtAIR12-Fw: CATGTCCCTGTGTCTTAAATA; AtAIR12-Rev: TGCAAGCCTGTTGTGAAATC; Ubq5-Fw: GTTAAGCTCGCTGTTCTTCAGT; Ubq5-Rev: TCAAGCTTCAACTCTTCTTTC.

Real-time PCR analysis was performed using a CFX96 Real-Time System (Biorad). One microliter of cDNA (corresponding to 50 ng of total RNA) was amplified in a 20  $\mu\text{l}$  reaction mix containing 1X JumpStarTaqReadyMix (Sigma) and 0.6  $\mu\text{M}$  of each primer.

For PAD3, total RNA was extracted from three independent biological replicates, each composed by 5 leaves. Three technical replicates were performed for each sample, and data analysis was done using the LinRegPCR software. Expression of PAD3 gene (At3g26830), relative to UBQ5, was determined using a modification of the Pfaffl method [49] as previously described [50]. Primers for analysis of PAD3 and UBQ5 transcripts were the following: Pad3-Fw: TCGCTGGCATAACACTATGG; Pad3-Rev: TTGGGAGCAAGAGTGGAGTT; Ubq5-Fw: GTTAAGCTCGCTGTTCTTCAGT; Ubq5-Rev: TCAAGCTTCAACTCTTCTTTC.

#### 2.9. Infection of leaves with *B. cinerea*

*B. cinerea* growth assays were performed on detached leaves as previously described [51]. Rosette leaves from 4-week-old, soil-grown *Arabidopsis* plants were placed in Petri dishes containing 0.8% agar, with the petiole embedded in the medium. Inoculation was performed by placing 5  $\mu\text{l}$  of a suspension of  $5 \times 10^5$  conidiospores/mL in 24 g/L potato dextrose broth (PDB) on each side of the middle vein. The plates were incubated at 22 °C with a 12 h photoperiod. High humidity was maintained by covering the plates with a clear plastic lid. Lesion size was determined by measuring the diameter or, in case of oval lesions, the axes of the necrotic area.

#### 2.10. Hydroxyl radicals (OH•) detection by electron paramagnetic resonance spectroscopy

Seedlings were grown on damped paper in the dark for 5 days. Spin-trapping assays were performed with the spin trap 4-pyridyl-1-oxide-N-tert-butylnitron (4-POBN) [52]. For each



sample, 30 seedlings were incubated for 4 h in 10 mM phosphate buffer (pH 6.0) in the presence of 50 mM 4-POBN, 4% ethanol. Electron paramagnetic resonance (EPR) spectra were recorded at 20 °C using an ESP 300 spectrometer (Bruker, Rheinstetten, Germany). The following parameters were used: microwave frequency 9.73 GHz, modulation frequency 100 kHz, modulation amplitude 1 G, microwave power 6.3 mW, receiver gain  $2 \times 10^4$ , time constant 40.96 ms, number of scans 4.

#### 2.11. Detection of superoxide with nitroblue tetrazolium

Accumulation of superoxide in leaves was detected via nitroblue tetrazolium (NBT) staining. Four-week-old plants were soaked for 3 h at room temperature in 50 mM K-phosphate buffer, pH 7.5, in the presence of 0.1% Triton X-100 and 0.025% NBT. After staining, leaves were bleached in 80% boiling ethanol, detached and placed on a transparency film. Intensity of the blue formazan precipitate was evaluated by three independent observers according to a predetermined scale (Fig. S1).

#### 2.12. Luminol-based assay for detection of hydrogen peroxide

Twelve leaf discs (0.125 cm<sup>2</sup>) from 5-week-old plants were incubated overnight in sterile water in a 96-well titer plate (Thermo Scientific NUNC), using one disk per well. ROS production was measured by a luminol-based assay in an aqueous solution containing 30 µg/mL luminol (Sigma–Aldrich) and 20 µg/mL type VI-A horseradish peroxidase (Sigma–Aldrich). Luminescence, recorded as total photon count during 40 min and expressed in relative light units (RLUs), was measured by using a GloMax 96 microplate luminometer with dual injectors (Promega) and signal integration time of 1 s.

#### 2.13. Lipid peroxidation

Lipid peroxidation in leaves was measured in 4-week-old plants by 2-thiobarbituric acid (TBA) test, as described in Ref. [53]. Briefly, different amounts (from 150 to 500 µg) of liquid nitrogen powdered leaves were vigorously mixed with 3 volumes of 0.1% trichloroacetic acid. Samples were centrifuged and 0.5 mL of supernatant was transferred into screw cap tubes in the presence of 2.0 mL 20% TCA and 1.5 µl 0.5% TBA. Following 30 min incubation at 90 °C, the reaction was stopped by placing the tubes on ice. The samples were centrifuged and the absorbance of the supernatant was read at 532 nm, subtracting the non-specific absorption at 600 nm. The amount of malondialdehyde–TBA complex was calculated using an extinction coefficient of 155 mM<sup>−1</sup> cm<sup>−1</sup>.

#### 2.14. Generation of AIR12-promoter YFP and GUS lines

The YFP (Yellow Fluorescent Protein)-coding sequence and the GUS (β-glucuronidase)-coding sequence were both fused to the Arabidopsis AIR12 promoter (promAIR12; base positions −1554 to −1). The 1554 bp promoter fragment was amplified by PCR using genomic DNA extracted from Arabidopsis leaves as a template. The pair of primers, both carrying an EcoRI restriction site (underlined), was as follows: forward primer 5′-CATGGAATTCTGACCGAGAGATATTCAGTTCA-3′ and reverse primer 5′-CATGGAATTCGTGATGTTATATAGAAGGGCAATG-3′. After digestion, the promoter was cloned upstream of GUS or YFP coding regions into a modified pGreen0029 binary vector [43,54], where the GUS or YFP coding sequences, fused with the *nos* terminator, were previously inserted in the polylinker between *KpnI*–*SacI* restriction sites. The pGreen-promAIR12::GUS or pGreen-promAIR12::YFP constructs were transferred into GV3101-pSoup Agrobacterium strain [43] and Arabidopsis plants

(Col-0) were transformed by floral dip method [44] and screened on half-strength MS agar medium containing 50 µg/mL kanamycin. The presence of the insertions was confirmed by PCR on genomic DNA with the following specific primers: forward primer inside promAIR12 sequence: 5′-CTCACATTGCCACCTCTATAAT-3′; reverse primer inside the GUS coding sequence: 5′-GCCAACTGATCGTTAAACTGC-3′; reverse primer inside the YFP coding sequence 5′-CGGTGGTGCAGATGAAGTT-3′. Seven and three independent promAIR12::GUS and promAIR12::YFP T1 plants, respectively, were screened and selected for comparable expression of reporter genes. Subsequent work was conducted on T2 plants. Three independent GUS and YFP selected lines were used for the experiments. The data shown are the most representative ones.

For experiments of AIR12 promoter activity during seedling development, seeds of Arabidopsis promAIR12::GUS and promAIR12::YFP were vapour-phase sterilized and placed in plates containing half-strength MS medium including 0.8% agar. The medium was enriched with 0.1% sucrose and 0.05% MES. After cold treatment for 2–3 days the plates were exposed to 16/8 h cycles of white light ( $\sim 75 \mu\text{E m}^{-2} \text{s}^{-1}$ ) in the growth chamber at 24 °C.

Histochemical GUS assays, and YFP detection was performed as previously described [54]. For experiments of plasmolysis, leaf epidermal strips of AIR12-oe plants were prepared as previously [42] and bathed first in milliQ water, and then perfused with 250 mM of sorbitol. Images were acquired with 10 s intervals, with an inverted Leica SP5 confocal microscope (Leica, Germany) in the XYT mode configuration.

### 3. Results

#### 3.1. AIR12 is associated with the plasma membrane

Sequences encoding AIR12 are exclusively found in genomes of flowering plants. AIR12 invariably contains a predicted N-terminal signal peptide for translocation into the endoplasmic reticulum and a GPI-modification sequence in the C-terminal part of the protein [28]. Following translocation along the secretion pathway, GPI-proteins are typically found associated with the external leaflet of the plasma membrane and/or with the cell wall.

An ascorbate-reducible cytochrome *b*, later identified as AIR12 [28], was shown to be bound to the plasma membrane by isopycnic centrifugation on sucrose gradients of membrane vesicles from etiolated hypocotyls of soybean (*Glycine max*) [30]. In order to verify the *in vivo* localization of AIR12 from *Glycine max* (GmAIR12) with a different experimental approach, a construct was prepared in which the YFP coding sequence was inserted between the N-terminal signal peptide and the coding sequence of GmAIR12 (Fig. 1A). The construct was placed under the control of a double 35S promoter and used for stable transformation of Arabidopsis [ecotype Landsberg erecta (Ler-0)], obtaining YFP-GmAIR12-expressing plants. Successful expression of the transgene was demonstrated by RT-PCR (Fig. 1B).

Fluorescence detected in leaves of YFP-GmAIR12-expressing plants nicely matched the boundaries of leaf epidermal cells (Fig. 1C–E). Following hyperosmotic treatment, part of the fluorescence signal followed the contraction of plasmolyzed protoplasts (compare Fig. 1F–H, before plasmolysis, with Fig. 1I–M, after plasmolysis; see also Supplementary Video 1). Given the hydrophilic nature of AIR12, it is plausible that its physical association to the plasma membrane is guaranteed by the GPI anchor, in agreement with proteomic studies [38,55].

Hereon, we will refer to plants expressing the YFP-GmAIR12 construct under the control of the double 35S promoter as GmAIR12-overexpressing plants (GmAIR12-oe).

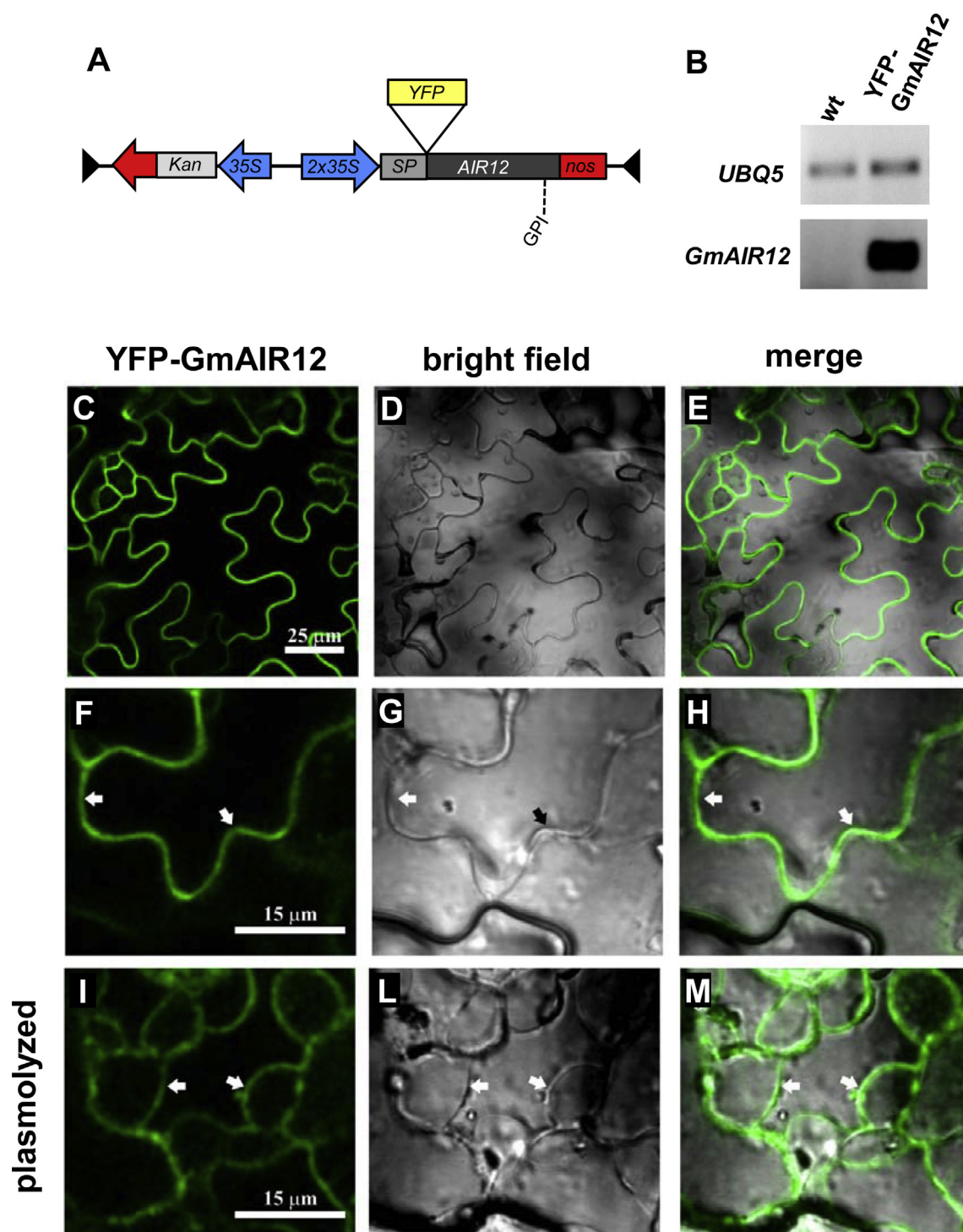


**Fig. 1.** Soybean AIR12 is targeted to the plasma membrane in transgenic Arabidopsis plants. Panel A: Schematic representation of the construct used for expression of YFP-GmAIR12 in Arabidopsis ecotype Ler-0 (SP, signal peptide). Panel B: Expression of *GmAIR12* gene in YFP-GmAIR12-transformed Arabidopsis plants. RT-PCR analysis was performed using cDNA (50 ng) obtained from total RNA extracted from 4-weeks adult plants. The expression of the house-keeping gene ubiquitin-5 (*UBQ5*) was determined as a control. Panels C–E: Localization of YFP-GmAIR12 fluorescence in leaf epidermal cells of transgenic Arabidopsis plants. Panels F–M: Magnification of an epidermal cell before (F–H) and after treatment with 250 mM sorbitol to induce plasmolysis (I–M). White arrows indicate portions of the fluorescent plasma membrane detaching from the cell wall upon plasmolysis.

3.2. *AIR12* is a b-type cytochrome reacting with both ascorbate/monodehydroascorbate and superoxide/oxygen redox couples

*Arabidopsis thaliana* contains a single *AIR12* gene (At3g07390), encoding a predicted mature protein that is 38% identical (54%

similar) to *Glycine max* *AIR12* [28]. With the aim of studying its biochemical properties, a recombinant form of Arabidopsis *AIR12* was obtained using *Pichia pastoris* as a heterologous expression system. A stop codon was introduced immediately upstream of the GPI-modification site in order to obtain a soluble form of the protein (sAIR12) with no GPI-anchor. Purified sAIR12, obtained

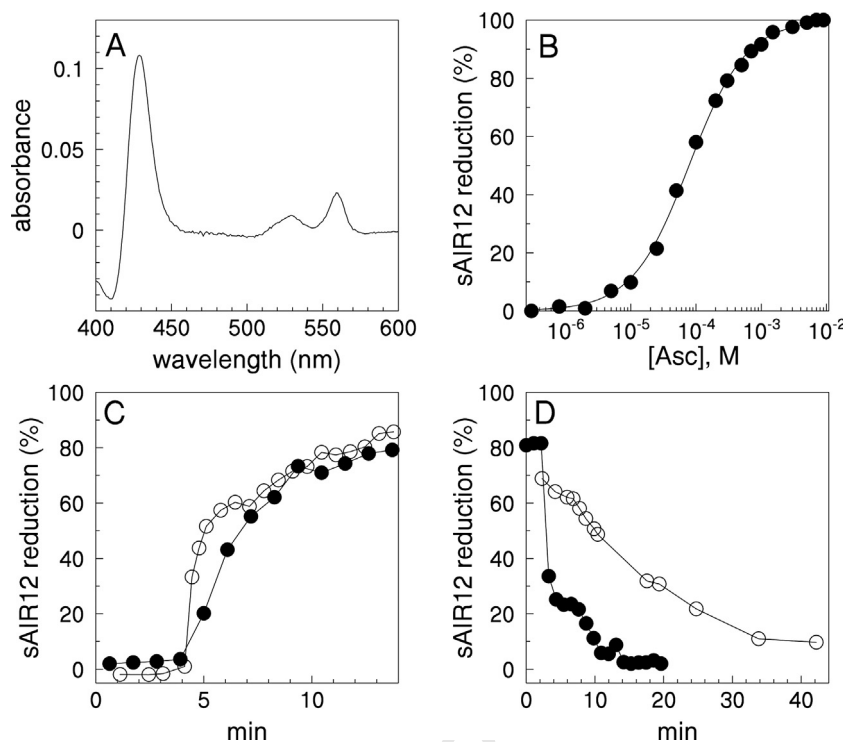


**Fig. 2.** Biochemical properties of recombinant sAIR12 from *Arabidopsis thaliana*. (A) Dithionite-reduced-minus-oxidized spectrum of purified sAIR12 (2  $\mu$ M) shows typical features of a *b*-type cytochrome. The  $\gamma$ -,  $\beta$ - and  $\alpha$ -bands were at 429, 530 and 560 nm, respectively. (B) Concentration-dependent reduction of sAIR12 (2  $\mu$ M) by Asc at pH 5.5. Experimental points were interpolated by non linear regression with a sigmoidal equation. (C) Time-dependent reduction of sAIR12 (1  $\mu$ M) by 1 mM Asc (closed circles, pH 5.5), or superoxide generated by xanthine (1 mM) plus xanthine oxidase (0.2 units/mL) (open circles, pH 7.0). Additions of Asc or xanthine oxidase were at minute 4. (D) Time-dependent oxidation of reduced sAIR12 by MDHA generated by Asc (0.6 mM) plus Asc oxidase (1 unit/mL) (closed circles, pH 5.5), added after 4 min of measurement. To detect sAIR12 autooxidation, Asc-reduced sAIR12 was gel-filtrated to remove the reductant and its reduction state immediately monitored over time in an open cuvette (open circles, pH 5.5). The reduced state of sAIR12 (panels B–D) was calculated from reduced-minus-oxidized spectra of the  $\alpha$ -band. For normalization, 100% reduction was obtained with dithionite addition.

as previously described for GmAIR12 [28], was found to be glycosylated, and treatment with endoglycosidase-H generated a 22 kDa band in SDS-PAGE corresponding to deglycosylated sAIR12 (theoretical molecular mass 21.8 kDa; Fig. S2).

Purified sAIR12 had typical spectral properties of a *b*-type cytochrome (Fig. 2A) with a symmetric  $\alpha$ -band at 560 nm (reduced-minus-oxidized). The cytochrome was half-reduced by 80  $\mu$ M Asc and fully reduced by Asc concentrations exceeding 10 mM (Fig. 2B). The single inflection point of Asc-dependent titrations (Fig. 2B) was consistent with the presence of a single heme, as previously found in *Glycine max* AIR12 [28]. As an alternative to Asc, superoxide produced by a xanthine/xanthine oxidase system could also reduce sAIR12 very efficiently (Fig. 2C). On the other hand, reduced sAIR12 was insensitive to hydrogen peroxide (not shown), slowly oxidized by oxygen and rapidly oxidized by MDHA generated by an Asc/Asc oxidase system (Fig. 2D). Based on its single heme, reduced sAIR12 is likely to perform 1-electron reactions, i.e. Asc regeneration from MDHA reduction, or production of superoxide ( $O_2^{\cdot-}$ ) from oxygen reduction. *Arabidopsis* AIR12 is thus a PM-associated cytochrome able to interact with common redox couples of the apoplast such as MDHA/Asc and  $O_2/O_2^{\cdot-}$ . Notably, several biochemical features of AIR12 from *Arabidopsis thaliana* match those of AIR12 from *Glycine max* [28,30].

### 3.3. *Arabidopsis* mutants with increased or decreased expression of AIR12 show no obvious phenotype under normal conditions

With the aim of investigating the physiological role of AIR12, an *Arabidopsis* Ler-0 mutant line carrying an insertion in the single exon of AIR12 was obtained from the CSHL collection (ET8602). A homozygous AIR12 knock-out line (AIR12-ko) was selected by PCR

on genomic DNA and the absence of AIR12-transcript was demonstrated by RT-PCR, using gene specific primers annealing at the 5'- and at 3'-end of the AIR12 coding sequence (Fig. S3). In order to generate AIR12 complemented plants (AIR12-comp), the AIR12-ko mutant was transformed with a 2802 bp genomic fragment, composed by the promoter region of AIR12, the AIR12 coding sequence and a 426 bp fragment located downstream the stop codon. RNAs extracted from WT, AIR12-comp and GmAIR12-oe plants were analyzed by RT-PCR with specific primers amplifying a 152 bp region of *Arabidopsis* AIR12 (Fig. S4). In both AIR12-comp plants and plants overexpressing soybean AIR12 (GmAIR12-oe), transcript levels of *Arabidopsis* AIR12 were similar to wild type levels.

None of these mutant plants showed obvious phenotypic alterations under control growth conditions at any developmental stage.

### 3.4. High levels of AIR12 expression lead to higher levels of reactive oxygen species

With the aim of elucidating whether an altered expression of AIR12 leads to an altered production of reactive oxygen species (ROS) and related compounds, we analyzed the levels of hydroxyl radical ( $OH^{\cdot}$ ), superoxide ( $O_2^{\cdot-}$ ), hydrogen peroxide ( $H_2O_2$ ) and lipid peroxides (L-OOH) in the different AIR12 mutant genotypes compared with wild-type plants.

Hydroxyl radicals were determined *in vivo* by EPR, using 5-day-old etiolated seedlings because of technical constraints intrinsic to this type of assay. Results showed no significant differences among the four different genotypes (Fig. 3A). Basal levels of superoxide were determined by NBT staining in rosette leaves of 4-week-old plants (Fig. 3B). Based on this assay, GmAIR12-oe showed higher superoxide levels than wild-type plants, while



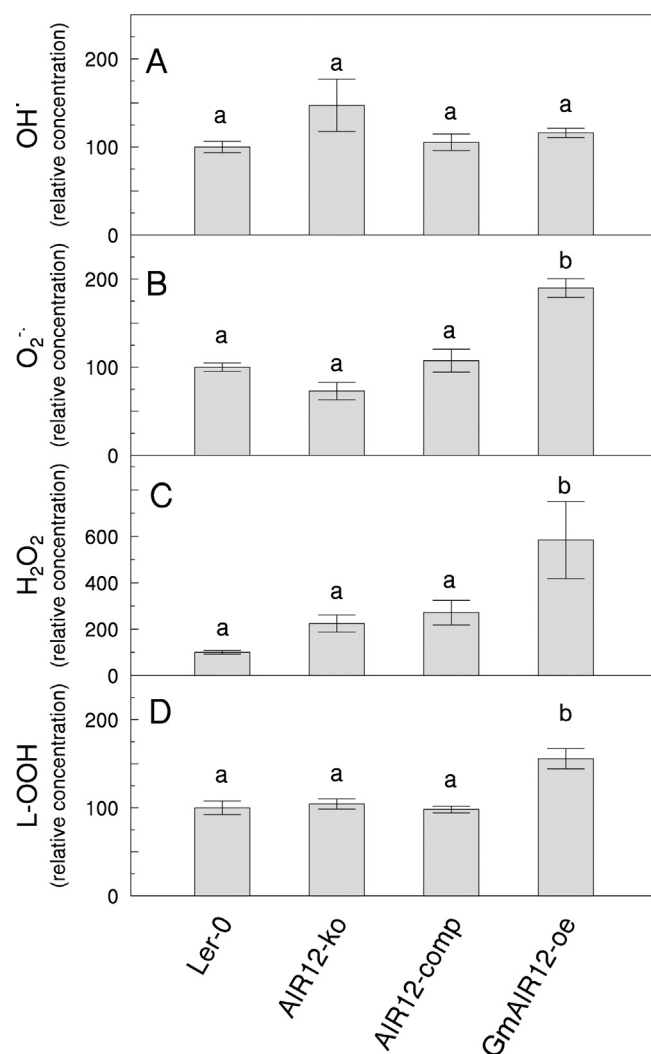


**Fig. 3.** Relative amounts of ROS and lipid peroxidation in different genotypes of Arabidopsis with different expression levels of AIR12. All values are normalized to the corresponding wild type values. (A) Hydroxyl radical ( $\text{OH}^\bullet$ ) was determined by Electron paramagnetic resonance (EPR) spectroscopy. Five-days-old etiolated seedlings (25 for each measure) were incubated with the spin trap reagent and spectra recorded in the incubation medium. Values are means  $\pm$  SE of 4 independent measures for each genotype. (B) Relative superoxide ( $\text{O}_2^{\bullet-}$ ) levels in leaves of 4-week-old plants as determined by the NBT assay. Intensity of the blue staining (formazan) was visually quantified according to a predetermined scale. At least 100 leaves of each genotype were analyzed by three independent observers ( $n=3$ ). Data shown are means  $\pm$  SE. (C) Hydrogen peroxide levels in leaf discs of 5-week-old plants were determined through a luminol-based assay. Six leaf discs for each genotype were individually analyzed. Luminescence was recorded as total photon count during 40 min. Data shown are means  $\pm$  SE. (D) Thiobarbituric acid-reactive-substances in whole leaves, 3 samples analyzed for each genotype. Data shown are means  $\pm$  SE. The actual value of Ler-0 samples was  $2.08 \pm 0.16$  nmol malondialdehyde-TBA complex per gram fresh weight. Statistical analysis was performed using ANOVA with LSD test for means comparison,  $P < 0.01$  (CoHort software).

no differences were observed in either AIR12-ko or AIR12-comp mutants. Determination of  $\text{H}_2\text{O}_2$  in leaf discs by a luminol-based assay (Fig. 3C) gave results resembling those obtained with NBT staining of whole leaves. A higher level of  $\text{H}_2\text{O}_2$  was detected in GmAIR12-oe leaf discs, while both AIR12-ko and AIR12-comp genotypes behaved similarly to the wild type (Fig. 3C). Finally, lipid peroxidation analyses, performed via thiobarbituric acid-reactive-substances (TBARS) assay, also provided significantly higher values in GmAIR12-oe plants than in other genotypes (Fig. 3D). Taken together these data suggest that high levels of expression of AIR12 may alter the plant redox state, as indicated by the higher levels of

superoxide, hydrogen peroxide and lipid peroxides in GmAIR12-oe plants, implying that AIR12 may play a pro-oxidant role *in vivo*. However, in AIR12-ko plants no significant decrease of any type of ROS was determined, suggesting that in wild type plants AIR12 provides a limited contribution to basal ROS levels.

### 3.5. The expression pattern of AIR12 in Arabidopsis plants suggest a correlation with cell separation

In order to investigate whether expression of AIR12 is regulated, the expression profile of the promoter (promAIR12) was studied during development. Just after completion of the germination process, seeds of promAIR12::GUS plants displayed a strong signal in the micropilar endosperm, a living tissue in which cells are actively separated to open the way to the emerging radicle (Fig. 4A). In seedlings, promAIR12 activity was first detected in developing veins of cotyledons, in stipules and primary leaf primordia (Fig. 4B and C). Expression in roots was mostly associated to root turns and sites of lateral root initiation (Fig. 4D–N). Detailed analysis of promAIR12::YFP seedlings roots clearly indicated that AIR12 expression was mostly confined to the root cap and few cells surrounding lateral roots. In adult plants, the expression of AIR12 was irregularly distributed in leaves (Fig. 4O), but also associated to the base of trichomes (Fig. 4P). AIR12 was also expressed in flowers, particularly in the abscission zone of floral organs (Fig. 4Q). Many of the sites where AIR12 expression is stronger correspond to sites where cell walls are actively separated during plant development [56]. In particular, the micropilar endosperm during germination, the sites of lateral root emergence, the root cap and the abscission zones of floral organs.

### 3.6. AIR12-ko mutants display lower susceptibility to *B. cinerea* infection

Since the capability of necrotrophic pathogens to colonize the host is strongly influenced by the redox state of the apoplast [17], a feature that seems to be modified in plants with altered levels of AIR12, leaves of four-week-old plants of the above described AIR12 mutants were infected with spores of *B. cinerea*. Two days after inoculation, wild type plants (Ler-0) displayed rapidly expanding water-soaked lesions, while the lesions of AIR12-ko plants were significantly smaller in size (40% of wild type,  $P < 0.05$ ; Fig. 5). The size of the lesions in AIR12-comp plants was intermediate between AIR12-ko and Ler-0 plants. Lesions of GmAIR12-oe plants were not statistically different from those of the wild type. These data show that absence of AIR12 leads to increased resistance to *B. cinerea* in Arabidopsis plants.

Whether the resistant phenotype of GmAIR12-ko plants depended on the constitutive induction of PHYTOALEXIN DEFICIENT 3 (PAD3) gene was evaluated by real time-PCR (Fig. S5). PAD3 encodes a cytochrome P450 CYP71B15 that catalyzes the last step of the biosynthesis of the phytoalexin camalexin, which is known to contribute to Arabidopsis basal resistance to *B. cinerea* [57]. However, no clear correlation was observed between PAD3 expression and resistance to Botrytis in the different genotypes analyzed in this work. PAD3 expression was higher in GmAIR12-oe, but not different from the wild type in the other genotypes (Fig. S5), suggesting that PAD3 might not be involved in the resistance to *B. cinerea* observed in AIR12-ko plants.

### 3.7. AIR12 promoter activity in Arabidopsis leaves is activated by *B. cinerea* infection and wounding

Given that the spread of *B. cinerea* in leaves is hindered by the absence of AIR12 (Fig. 5), we asked whether the pathogen might affect AIR12 gene expression. In leaves at a similar developmental

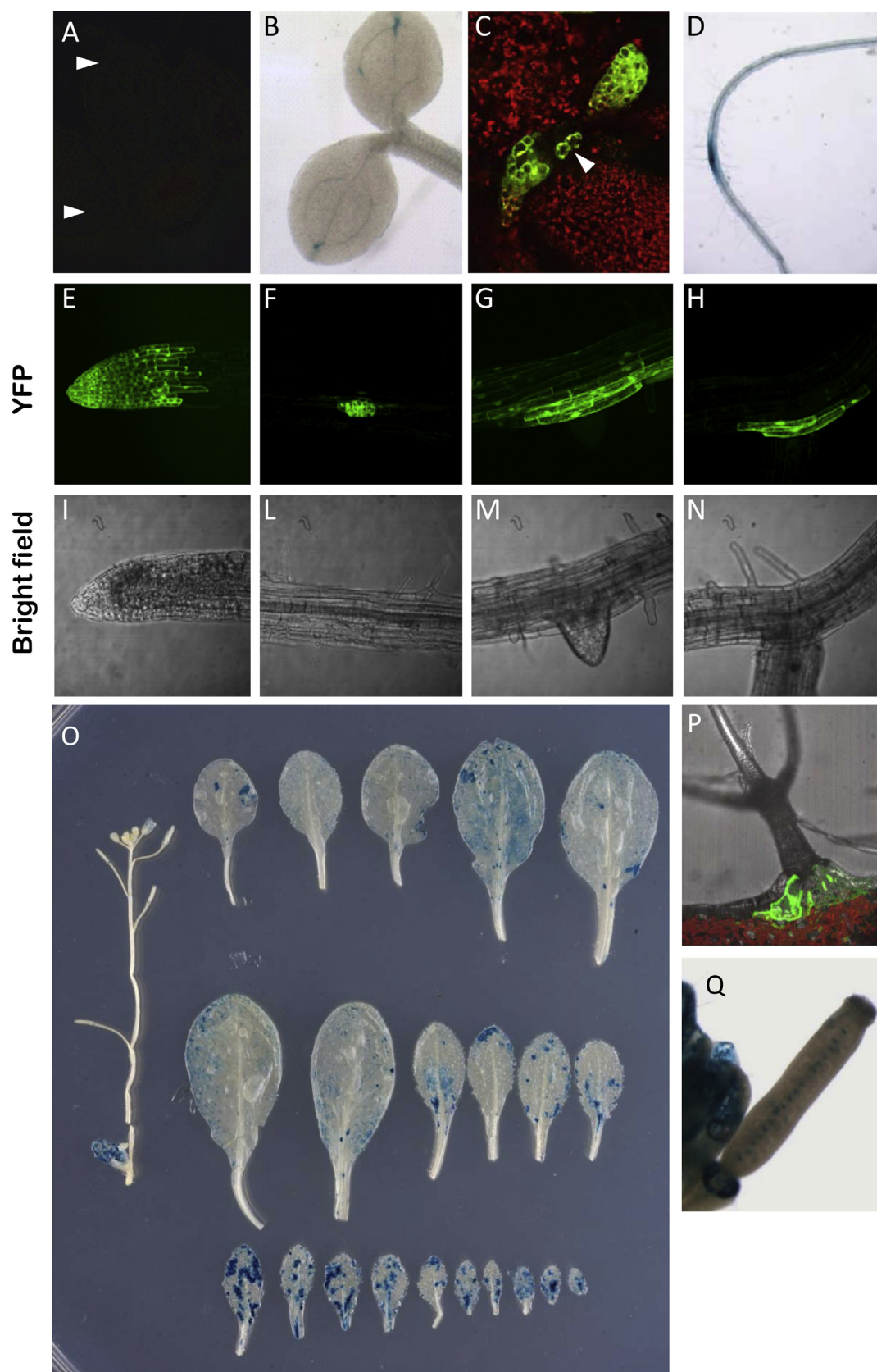


**Fig. 4.** Localized expression of AIR12 as shown by detailed analysis of Arabidopsis transgenic plants expressing either the GUS reporter or the YFP reporter, under the control of the *AIR12* promoter (promAIR12). (A) Imbibed seeds before and after radicle emergence (GUS staining). Arrowheads indicate the micropilar endosperm. (B) Cotyledons of 2-day-old seedling (GUS). (C) Stipules (arrowhead) and primary leaf primordia in a 7-day-old seedling (merge of YFP and red chlorophyll fluorescence). (D) Seedling root turn (GUS staining). Panels E–N: 7-Day-old seedling roots (YFP and bright field): panels E/I, root apex; F, L, G, M, H, N, sites of lateral root emergence at different developmental stages. O: leaves and inflorescence of a 4-week-old plant (GUS staining); the oldest leaf in the upper left and the youngest leaf in the bottom right. P: trichome (merge of YFP, red chlorophyll fluorescence and bright field). Q: developing silique after shedding of sepals and petals (GUS staining).



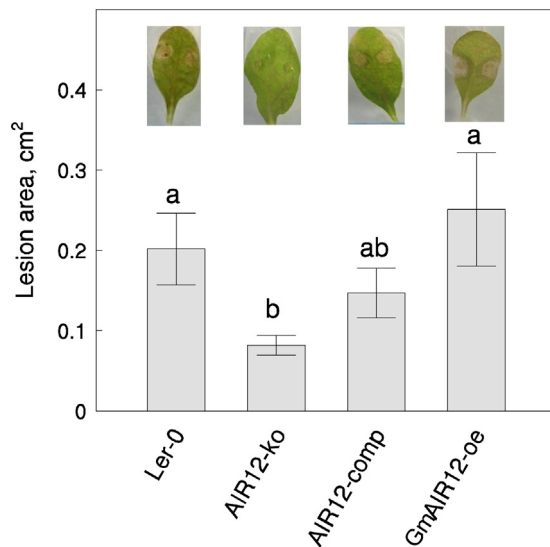


**Fig. 5.** AIR12 negatively regulates resistance to *B. cinerea* infection in Arabidopsis. Lesion area was measured 48 h post-infection in 20 leaves of each genotype. Data are means  $\pm$  SE. Statistical analysis was performed using ANOVA with LSD test for means comparison,  $P < 0.05$ . One representative infected leaf is shown for each genotype.

stage as those used in *B. cinerea* infection experiments, the promoter activity of *AIR12* was very weak. However, the infection with *B. cinerea* spores induced a clear increase of *promAIR12* activity, both in the sites of infection and in distant portions of the leaf, particularly in the vascular system (Fig. 6). Thirty-six hours after inoculation, *AIR12* promoter activity was still high in the vascular tissue, but absent at infection sites, likely due to cell death.

Expression of *AIR12* was also strongly induced by wounding. In leaves, *promAIR12::GUS* activity started to be induced 3-h after wounding, and increased at later time points (6 and 24-h), spreading also beyond the wound (Fig. 7).

#### 4. Discussion

*AIR12* is a cytochrome *b* [28] and as such it can perform several redox reactions. Here we show that *in vitro* *AIR12* can be reduced by Asc or by superoxide, and be oxidized by MDHA or oxygen, although the interaction with other, still unknown, redox compounds cannot be excluded. *AIR12* is a hydrophilic protein that was shown to be glycosylated *in planta* [29] and when expressed in *Pichia pastoris* [28], and is predicted to bear a GPI-modification for membrane anchoring. The previously suggested association of *AIR12* to the plasma membrane [30] is here conclusively demonstrated in Arabidopsis plants that constitutively express a YFP-*AIR12* fusion protein. Proteomic studies further supported the plasma membrane localization [58,59] and the GPI-modification of *AIR12* in several plants [31,33,55]. As a glycosylated, hydrophilic and GPI-anchored plasma membrane protein, *AIR12* is predicted to be exposed toward the apoplast [60] where it might perform its redox activity.

To get insights about how *AIR12* might modify the apoplastic environment *in vivo*, the production of different types of ROS ( $O_2^{\cdot-}$ ,  $H_2O_2$ ,  $OH^{\cdot}$ ) and ROS-related compounds (lipid peroxides) was analyzed in Arabidopsis mutants with altered levels of *AIR12* expression. *AIR12* overexpressing plants consistently showed higher levels of each type of ROS, a result apparently consistent with the *in vitro* capability of reduced *AIR12* to convert oxygen to superoxide. However, loss of *AIR12* function in *AIR12* knock out plants did not correspond to significantly lower levels of ROS. This observation suggests that, in the complex network of reactions that

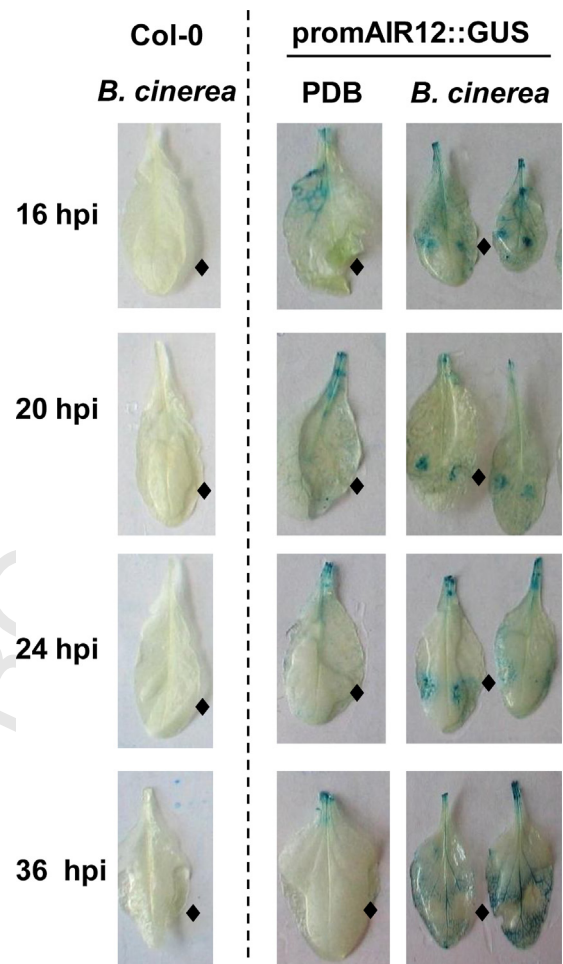


**Fig. 6.** Induction of *AIR12* promoter activity after infection with *B. cinerea*. Detached leaves of 4-week-old wild-type and *promAIR12::GUS* plants were inoculated with a suspension of conidiospores of *B. cinerea* on each side of the middle vein in the apical portion of the leaves (see diamonds). GUS staining was performed at 16, 20, 24 and 36 h post-inoculation (hpi). PDB, Potato Dextrose Broth (mock inoculation).

regulate ROS levels *in vivo*, *AIR12* does not play a major role in most tissues under normal conditions. This hypothesis does not exclude the possibility of a role of this redox protein in specific cells and at specific developmental stages, as actually suggested by the regulated expression of the gene in particular sites of the plant in which cell walls undergo separation, as discussed below.

*AIR12* belongs to the large superfamily of DOMON proteins [35]. Some DOMON proteins, like *AIR12*, bind a heme and perform redox reactions [61]. Besides *AIR12*, plants contain a large family of proteins in which a trans-membrane CYB561 domain [34] is fused to an extra-cellular DOMON domain. These proteins have been named CYBDOMs [20]. CYBDOMs are predicted to bind three hemes *b* (two in CYB561, one in the DOMON) and constitute an electron route across the plasma membrane from cytosolic ascorbate to the cell wall [20,36]. The very existence of CYBDOMs suggests that *AIR12* and CYB561 may interact *in vivo* [62]. Consistently, both *AIR12* and CYB561s and CYBDOMs have been found associated to lipid rafts in several systems [37–40]. Although the link between the redox activity of *AIR12* and its function *in vivo* is still unknown, here we show that loss of *AIR12* affects the plant response to *B. cinerea*. This result is in agreement with the notion that redox conditions of the apoplast are important for the pathogenesis of necrotrophic pathogens [17]. In the initial stage of infection, *B. cinerea*, like *Sclerotinia sclerotiorum*, secretes oxalate to inhibit the plant oxygen burst [14,16] and creates less oxidizing conditions

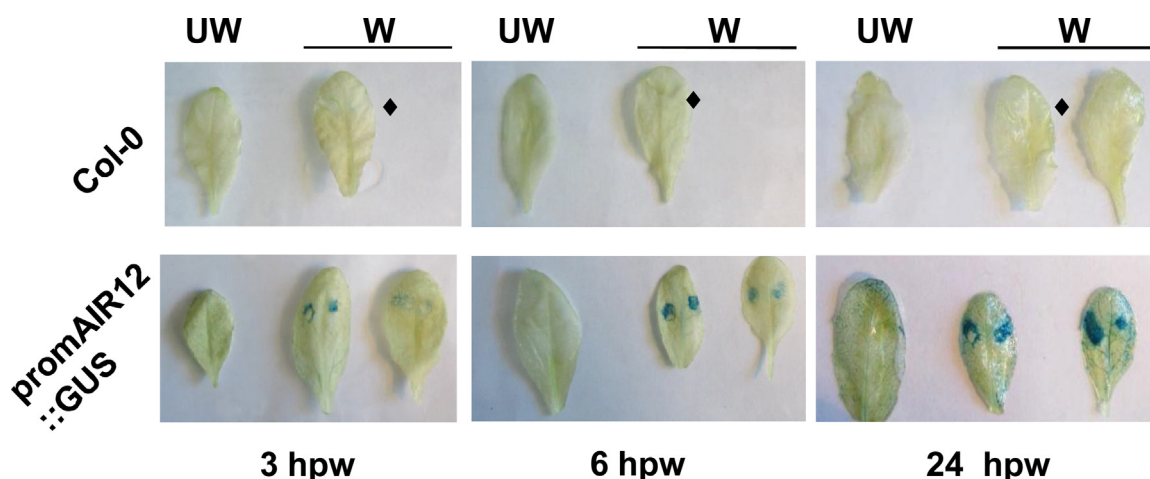


**Fig. 7.** Induction of AIR12 promoter activity by wounding. Leaves of 4-week-old plants were wounded by forceps on each side of the middle vein in the apical portion of the leaves (see diamonds). At 3, 6 and 24 h post-wounding (hpw), GUS staining was performed. Data from one representative promAIR12::GUS line is shown; a second independent line showed a similar response. UW, unwounded; W, wounded.

that inhibit plant defence responses (e.g. cross-linking reactions and lignin deposition) and favor pathogen invasion [15]. However, once the infection is established, induction of the plant oxidative burst triggers programmed cell death in the host tissue, favoring *B. cinerea* proliferation on dead cells [17]. We have found that the AIR12 loss-of-function mutant has increased resistance to *B. cinerea*. Thus AIR12, the expression of which is strongly induced by *B. cinerea* itself, functions as a susceptibility factor in the interaction with this fungus, likely contributing to the oxidative load in the infected tissues that promotes *B. cinerea* growth and disease development. On the other hand, the fact that transgenic overexpression of soybean AIR12 in Arabidopsis plants (GmAIR12-oe) does not lead to increased susceptibility may indicate that the level of ROS produced by AIR12 during infection of wild type plants is already optimal for *B. cinerea*, and/or that a further increase of ROS is compensated by other plant defense responses.

GPI-anchored proteins constitute about 0.5% of the plant proteome [35,55] and are largely represented by proteins involved in cell wall remodeling [33]. GPI-proteins also represent a predominant portion of the proteins associated to lipid rafts [32,56]. In mammalian cells, it was shown that the GPI anchor is one of the signals targeting a protein to lipid rafts and that GPI-proteins specifically interact with sterol-rich membrane domains [62–65]. In Arabidopsis, lipid rafts are composed of a variable set of signaling proteins (e.g. receptor kinases, G-proteins, calcium signaling proteins) and a constant set of *ca.* 40 sterol-dependent proteins, including AIR12, most of which are GPI-anchored and involved in cell wall remodeling [38]. All these observations suggest a cell wall-related role for AIR12.

In line with a cell wall-related role of AIR12, other DOMON proteins have been shown to function in the modification/organization of the extracellular matrix, both in animals and fungi [61]. KNICKKOPF, a GPI-anchored DOMON-protein is involved in the correct organization of chitin microfibrils in insects and possibly all invertebrates with chitinous exoskeleton [66]. The DOMON-heme of KNICKKOPF is essential for its function in chitin organization [67]. Cellobiose dehydrogenase (CDH), a flavo-cytochrome secreted by several species of wood-degrading fungi does also contain a DOMON-heme and is involved in the degradation of ligno-cellulosic substrates [68]. Unfortunately, the catalytic mechanism of both CDH and KNICKKOPF is still little understood.

A role of AIR12 in cell wall remodeling is also compatible with its expression pattern throughout the plant. The AIR12 promoter show high activity in sites where cell walls are being separated

and modified: ruptured micropilar endosperm of germinated seeds, the base of trichomes, root cells separated by the emerging lateral root, floral organs abscission zones, and cells surrounding a wound. These sites may be associated with ROS production and/or cross-linking reactions in the cell wall [8,69–71]. However, AIR12 *per se* would not control any of these phenomena as AIR12-knock out plants did not show any obvious phenotype, apart from the decreased susceptibility to *B. cinerea*.

A subtle role of AIR12 in cell wall organization may also explain the altered response to the fungus. Modifications of cell wall architecture or composition have been shown to influence resistance against necrotrophic pathogens, including *B. cinerea* [15,16,72–81]. In some of the cell wall mutants, resistance relies on constitutive defense responses, including production of ROS and phytoalexins [82]. In our case, however, increased ROS levels and PAD3 expression are not clearly associated to the response.

Notably, it has been shown that necrotrophs can force plants to cooperate in disease by altering the host cell wall [83]. For example Arabidopsis AtPME3 (a pectin methylesterase) is induced upon infection with *B. cinerea* and functions as susceptibility factor [81,84]. AIR12 provides an additional example of how necrotrophs exploit the host cell wall metabolism to facilitate pathogenesis. An intriguing hypothesis, suggested by the similarities between AIR12 and cellobiose dehydrogenase [28,68,85] is that AIR12 may affect the structure of the plant ligno-cellulosic network. Such a function may be important in developmental processes that involve tissue rupture but also cell division and differentiation, including wound healing.

In conclusion, here we show that AIR12 is a redox-active protein predicted to face the apoplast, potentially able to affect the redox state of this compartment and in turn modify the cell wall. In healthy plants, AIR12 might function with its redox activity in cell separation processes that physiologically occur during development or upon mechanical injury. Low expression levels of AIR12 in Arabidopsis mutants are associated to low susceptibility to *B. cinerea*, pointing to a role as a negative regulator of resistance against this necrotrophic pathogen. Whether this effect is a consequence of the activity exerted by AIR12 on the cell wall needs to be elucidated.

#### Acknowledgment

This work was funded by the Ministero dell'Istruzione, dell'Università e della Ricerca (PRIN2009).

## Appendix A. Supplementary data

Supplementary data associated with this article can be found, in the online version, at <http://dx.doi.org/10.1016/j.plantsci.2015.01.004>.

## References

- [1] P. Albersheim, A. Darvill, K. Roberts, R. Sederoff, A. Staehelin, Plant Cell Walls, Garland Science/Taylor and Francis Group, New York, 2011.
- [2] R. Angelini, A. Cona, R. Federico, P. Fincato, P. Tavladoraki, A. Tisi, Plant amine oxidases on the move: an update, Plant Physiol. Biochem. 48 (2010) 560–564.
- [3] J.A. O'Brien, A. Daudi, V.S. Butt, G.P. Bolwell, Reactive oxygen species and their role in plant defence and cell wall metabolism, Planta 236 (2012) 765–779.
- [4] A. Baxter, R. Mittler, N. Suzuki, ROS as key players in plant stress signalling, J. Exp. Bot. 65 (2014) 1229–1240.
- [5] C. Pignocchi, G. Kiddle, I. Hernandez, S.J. Foster, A. Asensi, T. Taybi, J. Barnes, C.H. Foyer, Ascorbate oxidase-dependent changes in the redox state of the apoplast modulate gene transcript accumulation leading to modified hormone signaling and orchestration of defense processes in tobacco, Plant Physiol. 141 (2006) 423–435.
- [6] P. Schopfer, A. Liskay, Plasma membrane-generated reactive oxygen intermediates and their role in cell growth of plants, Biofactors 28 (2006) 73–81.
- [7] J.C. Dumville, S.C. Fry, Solubilisation of tomato fruit pectins by ascorbate: a possible non-enzymic mechanism of fruit softening, Planta 217 (2003) 951–961.
- [8] K. Muller, A. Linkies, R.A. Vreeburg, S.C. Fry, A. Krieger-Liszky, G. Leubner-Metzger, In vivo cell wall loosening by hydroxyl radicals during cress seed germination and elongation growth, Plant Physiol. 150 (2009) 1855–1865.
- [9] T. Engelsdorf, T. Hamann, An update on receptor-like kinase involvement in the maintenance of plant cell wall integrity, Ann. Bot. (2014), <http://dx.doi.org/10.1093/aob/mcu043>.
- [10] S. Ferrari, D.V. Savatin, F. Sicilia, G. Gramegna, F. Cervone, G. De Lorenzo, Oligogalacturonides: plant damage-associated molecular patterns and regulators of growth and development, Front. Plant Sci. 4 (2013) 49, <http://dx.doi.org/10.3389/fpls.2013.00049>.
- [11] G.J. Seifert, C. Blaukopf, Irritable walls: the plant extracellular matrix and signaling, Plant Physiol. 153 (2010) 467–478.
- [12] D. Wendehenne, Q.M. Gao, A. Kachroo, P. Kachroo, Free radical-mediated systemic immunity in plants, Curr. Opin. Plant Biol. 20 (2014) 127–134.
- [13] C. Scheler, J. Durner, J. Astier, Nitric oxide and reactive oxygen species in plant biotic interactions, Curr. Opin. Plant Biol. 16 (2013) 534–549.
- [14] B. Williams, M. Kabbage, H.J. Kim, R. Britt, M.B. Dickman, Tipping the balance: *Sclerotinia sclerotiorum* secreted oxalic acid suppresses host defenses by manipulating the host redox environment, PLOS Pathog. 7 (2011) e1002107.
- [15] B. Asselbergh, K. Curvers, S.C. Franca, K. Audenaert, M. Vuylsteke, F. Van Breusegem, M. Hofte, Resistance to *Botrytis cinerea* in sitiens, an abscisic acid-deficient tomato mutant, involves timely production of hydrogen peroxide and cell wall modifications in the epidermis, Plant Physiol. 144 (2007) 1863–1877.
- [16] F. L'Haridon, A. Besson-Bard, M. Binda, M. Serrano, E. Abou-Mansour, F. Balet, H.J. Schoonbeek, S. Hess, R. Mir, J. Leon, O. Lamotte, J.P. Mettraux, A permeable cuticle is associated with the release of reactive oxygen species and induction of innate immunity, PLOS Pathog. 7 (2011) e1002148.
- [17] T. Mengiste, Plant immunity to necrotrophs, Annu. Rev. Phytopathol. 50 (2012) 267–294.
- [18] G. Noctor, Metabolic signalling in defence and stress: the central roles of soluble redox couples, Plant Cell Environ. 29 (2006) 409–425.
- [19] F.L. Booker, K.O. Burkey, A.M. Jones, Re-evaluating the role of ascorbic acid and phenolic glycosides in ozone scavenging in the leaf apoplast of *Arabidopsis thaliana* L., Plant Cell Environ. 35 (2012) 1456–1466.
- [20] H. Asard, R. Barbaro, P. Trost, A. Bérczi, Cytochromes b561: ascorbate-mediated trans-membrane electron transport, Antioxid. Redox Signal. 19 (2013) 1026–1035.
- [21] P.L. Conklin, C. Barth, Ascorbic acid, a familiar small molecule intertwined in the response of plants to ozone, pathogens, and the onset of senescence, Plant Cell Environ. 27 (2004) 959–970.
- [22] G. Potters, N. Horemans, S. Bellone, R.J. Caubergs, P. Trost, Y. Guisez, H. Asard, Dehydroascorbate influences the plant cell cycle through a glutathione-independent reduction mechanism, Plant Physiol. 134 (2004) 1479–1487.
- [23] M.A. Green, S.C. Fry, Vitamin C degradation in plant cells via enzymatic hydrolysis of 4-O-oxalyl-L-threonate, Nature 433 (2005) 83–87.
- [24] M.C. de Pinto, L. De Gara, Changes in the ascorbate metabolism of apoplastic and symplastic spaces are associated with cell differentiation, J. Exp. Bot. 55 (2004) 2559–2569.
- [25] H.T. Parsons, S.C. Fry, Reactive oxygen species-induced release of intracellular ascorbate in plant cell-suspension cultures and evidence for pulsing of net release rate, New Phytol. 187 (2010) 332–342.
- [26] N. Horemans, C.H. Foyer, H. Asard, Transport and action of ascorbate at the plant plasma membrane, Trends Plant Sci. 5 (2000) 263–267.
- [27] L.W. Neuteboom, J.M. Ng, M. Kuyper, O.R. Clijdesdale, P.J. Hooykaas, B.J. van der Zaai, Isolation and characterization of cDNA clones corresponding with mRNAs that accumulate during auxin-induced lateral root formation, Plant Mol. Biol. 39 (1999) 273–287.
- [28] V. Preger, N. Tango, C. Marchand, S.D. Lemaire, D. Carbonera, M. Di Valentin, A. Costa, P. Pupillo, P. Trost, Auxin-responsive genes AIR12 code for a new family

- of plasma membrane b-type cytochromes specific to flowering plants, Plant Physiol. 150 (2009) 606–620.
- [29] P. Trost, A. Bérczi, F. Sparla, G. Sponza, B. Marzadori, H. Asard, P. Pupillo, Purification of cytochrome b-561 from bean hypocotyls plasma membrane. Evidence for the presence of two heme centers, Biochim. Biophys. Acta 1468 (2000) 1–5.
- [30] V. Preger, S. Scagliarini, P. Pupillo, P. Trost, Identification of an ascorbate-dependent cytochrome b of the tonoplast membrane sharing biochemical features with members of the cytochrome b561 family, Planta 220 (2005) 365–375.
- [31] G.H. Borner, K.S. Lilley, T.J. Stevens, P. Dupree, Identification of glycosylphosphatidylinositol-anchored proteins in Arabidopsis. A proteomic and genomic analysis, Plant Physiol. 132 (2003) 568–577.
- [32] F. Elortza, T.S. Nühse, L.J. Foster, A. Stensballe, S.C. Peck, O.N. Jensen, Proteomic analysis of glycosylphosphatidylinositol-anchored membrane proteins, Mol. Cell. Proteomics 2 (2003) 1261–1270.
- [33] E. Lalanne, D. Honys, A. Johnson, G.H. Borner, K.S. Lilley, P. Dupree, U. Grossniklaus, D. Twell, SETH1 and SETH2, two components of the glycosylphosphatidylinositol anchor biosynthetic pathway, are required for pollen germination and tube growth in Arabidopsis, Plant Cell 16 (2004) 229–240.
- [34] P. Lu, D. Ma, C. Yan, X. Gong, M. Du, Y. Shi, Structure and mechanism of a eukaryotic transmembrane ascorbate-dependent oxidoreductase, Proc. Natl. Acad. Sci. U. S. A. 111 (2014) 1813–1818.
- [35] L. Aravind, DOMON: an ancient extracellular domain in dopamine beta-monooxygenase and other proteins, Trends Biochem. Sci. 26 (2001) 524–526.
- [36] C. Picco, J. Scholz-Starke, A. Naso, V. Preger, F. Sparla, P. Trost, A. Carpaneto, How are cytochrome b561 electron currents controlled by membrane voltage and substrate availability? Antioxid. Redox Signal. 21 (2014) 384–391.
- [37] B. Lefebvre, F. Furt, M.A. Hartmann, L.V. Michaelson, J.P. Carde, F. Sargueil-Boiron, M. Rossignol, J.A. Napier, J. Cullimore, J.J. Bessoule, S. Mongrand, Characterization of lipid rafts from *Medicago truncatula* root plasma membranes: a proteomic study reveals the presence of a raft-associated redox system, Plant Physiol. 144 (2007) 402–418.
- [38] S. Kierszniowska, B. Seiwert, W.X. Schulze, Definition of Arabidopsis sterol-rich membrane microdomains by differential treatment with methyl-beta-cyclodextrin and quantitative proteomics, Mol. Cell. Proteomics 8 (2009) 612–623.
- [39] N.F. Keinath, S. Kierszniowska, J. Lorek, G. Bourdais, S.A. Kessler, H. Shimosato-Asano, U. Grossniklaus, W.X. Schulze, S. Robatzek, R. Panstruga, PAMP (pathogen-associated molecular pattern)-induced changes in plasma membrane compartmentalization reveal novel components of plant immunity, J. Biol. Chem. 285 (2010) 39140–39149.
- [40] R.A. Bhat, M. Miklis, E. Schmelzer, P. Schulze-Lefert, R. Panstruga, Recruitment and interaction dynamics of plant penetration resistance components in a plasma membrane microdomain, Proc. Natl. Acad. Sci. U. S. A. 102 (2005) 3135–3140.
- [41] B.S. Leach, J.F. Collawn, W.W. Fish, Behavior of glycopolypeptides with empirical molecular weight estimation methods. 1. In sodium dodecyl sulfate, Biochemistry 19 (1980) 5734–5741.
- [42] A. Costa, I. Drago, S. Behera, M. Zottini, P. Pizzo, J.I. Schroeder, T. Pozzan, F. Lo Schiavo, H<sub>2</sub>O<sub>2</sub> in plant peroxisomes: an in vivo analysis uncovers a Ca(2+)-dependent scavenging system, Plant J. 62 (2010) 760–772.
- [43] R.P. Hellens, E.A. Edwards, N.R. Leyland, S. Bean, P.M. Mullineaux, pGreen: a versatile and flexible binary Ti vector for Agrobacterium-mediated plant transformation, Plant Mol. Biol. 42 (2000) 819–832.
- [44] S.J. Clough, A.F. Bent, Floral dip: a simplified method for Agrobacterium-mediated transformation of *Arabidopsis thaliana*, Plant J. 16 (1998) 735–743.
- [45] T.N. Petersen, S. Brunak, G. von Heijne, H. Nielsen, SignalP 4.0: discriminating signal peptides from transmembrane regions, Nat. Methods 8 (2011) 785–786.
- [46] A.G. von Arnim, X.W. Deng, M.G. Stacey, Cloning vectors for the expression of green fluorescent protein fusion proteins in transgenic plants, Gene 221 (1998) 35–43.
- [47] B. Eisenhaber, P. Bork, F. Eisenhaber, Prediction of potential GPI-modification sites in proprotein sequences, J. Mol. Biol. 292 (1999) 741–758.
- [48] F. Sparla, L. Rotino, M.C. Valgimigli, P. Pupillo, P. Trost, Systemic resistance induced by benzothiadiazole in pear inoculated with the agent of fire blight (*Erwinia amylovora*), Sci. Hortic.-Amst. 101 (2004) 269–279.
- [49] M.W. Pfaffl, A new mathematical model for relative quantification in real-time RT-PCR, Nucleic Acids Res. 29 (2001) e45, <http://dx.doi.org/10.1093/nar/29.9.e45>.
- [50] S. Ferrari, R. Galletti, D. Vairo, F. Cervone, G. De Lorenzo, Antisense expression of the *Arabidopsis thaliana* ATGP1 gene reduces polygalacturonase-inhibiting protein accumulation and enhances susceptibility to *Botrytis cinerea*, Mol. Plant Microbe Interact. 19 (2006) 931–936.
- [51] S. Ferrari, R. Galletti, C. Denoux, G. De Lorenzo, F.M. Ausubel, J. Dewdney, Resistance to *Botrytis cinerea* induced in Arabidopsis by elicitors is independent of salicylic acid, ethylene, or jasmonate signaling but requires PHYTOALEXIN DEFICIENT3, Plant Physiol. 144 (2007) 367–379.
- [52] S. Renew, E. Heyno, P. Schopfer, A. Liskay, Sensitive detection and localization of hydroxyl radical production in cucumber roots and Arabidopsis seedlings by spin trapping electron paramagnetic resonance spectroscopy, Plant J. 44 (2005) 342–347.
- [53] L. Guidi, G. Bonghi, S. Ciompi, G.F. Soldatini, In *Vicia faba* leaves photoinhibition from ozone fumigation in light precedes a decrease in quantum yield of functional PSII centres, J. Plant Physiol. 154 (1999) 167–172.
- [54] C. Valerio, A. Costa, L. Marri, E. Issakidis-Bourguet, P. Pupillo, P. Trost, F. Sparla, Thioredoxin-regulated beta-amylase (BAM1) triggers diurnal starch



- degradation in guard cells, and in mesophyll cells under osmotic stress, J. Exp. Bot. 62 (2011) 545–555.
- [55] F. Elortza, S. Mohammed, J. Bunkenborg, L.J. Foster, T.S. Nühse, U. Brodbeck, S.C. Peck, O.N. Jensen, Modification-specific proteomics of plasma membrane proteins: identification and characterization of glycosylphosphatidylinositol-anchored proteins released upon phospholipase D treatment, J. Proteome Res. 5 (2006) 935–943.
- [56] J.A. Roberts, K.A. Elliott, Z.H. Gonzalez-Carranza, Abscission, dehiscence, and other cell separation processes, Annu. Rev. Plant Biol. 53 (2002) 131–158.
- [57] S. Ferrari, J.M. Plotnikova, G. De Lorenzo, F.M. Ausubel, Arabidopsis local resistance to *Botrytis cinerea* involves salicylic acid and camalexin and requires EDS4 and PAD2, but not SID2, EDS5 or PAD4, Plant J. 35 (2003) 193–205.
- [58] D. Hopff, S. Wienkoop, S. Lühthje, The plasma membrane proteome of maize roots grown under low and high iron conditions, J. Proteomics 91 (2013) 605–618.
- [59] Z. Zhang, P. Voothuluru, M. Yamaguchi, R.E. Sharp, S.C. Peck, Developmental distribution of the plasma membrane-enriched proteome in the maize primary root growth zone, Front. Plant Sci. 4 (2013) 33, <http://dx.doi.org/10.3389/fpls.2013.00033>.
- [60] S. Mayor, H. Riezman, Sorting GPI-anchored proteins, Nat. Rev. Mol. Cell Biol. 5 (2004) 110–120.
- [61] L.M. Iyer, V. Anantharaman, L. Aravind, The DOMON domains are involved in heme and sugar recognition, Bioinformatics 23 (2007) 2660–2664.
- [62] C.J. Marcotte, E.M. Marcotte, Predicting functional linkages from gene fusions with confidence, Appl. Bioinform. 1 (2002) 93–100.
- [63] J.M. Cordy, I. Hussain, C. Dingwall, N.M. Hooper, A.J. Turner, Exclusively targeting beta-secretase to lipid rafts by GPI-anchor addition up-regulates beta-site processing of the amyloid precursor protein, Proc. Natl. Acad. Sci. U. S. A. 100 (2003) 11735–11740.
- [64] D.A. Brown, J.K. Rose, Sorting of GPI-anchored proteins to glycolipid-enriched membrane subdomains during transport to the apical cell surface, Cell 68 (1992) 533–544.
- [65] D.F. Legler, M.A. Doucey, P. Schneider, L. Chapatte, F.C. Bender, C. Bron, Differential insertion of GPI-anchored GFPs into lipid rafts of live cells, FASEB J. 19 (2005) 73–75.
- [66] B. Moussian, E. Tang, A. Tønning, S. Helms, H. Schwarz, C. Nusslein-Volhard, A.E. Uv, *Drosophila* Knickkopf and retroactive are needed for epithelial tube growth and cuticle differentiation through their specific requirement for chitin filament organization, Development 133 (2006) 163–171.
- [67] K.S. Shaik, Y. Wang, L. Aravind, B. Moussian, The Knickkopf DOMON domain is essential for cuticle differentiation in *Drosophila melanogaster*, Arch. Insect. Biochem. 86 (2014) 100–106.
- [68] R. Ludwig, W. Harreither, F. Tasca, L. Gorton, Cellobiose dehydrogenase: a versatile catalyst for electrochemical applications, ChemPhysChem 11 (2010) 2674–2697.
- [69] L. Denness, J.F. McKenna, C. Segonzac, A. Wormit, P. Madhou, M. Bennett, J. Mansfield, C. Zipfel, T. Hamann, Cell wall damage-induced lignin biosynthesis is regulated by a reactive oxygen species and jasmonic acid-dependent process in *Arabidopsis*, Plant Physiol. 156 (2011) 1364–1374.
- [70] N. Suzuki, R. Mittler, Reactive oxygen species-dependent wound responses in animals and plants, Free Radic. Biol. Med. 53 (2012) 2269–2276.
- [71] E. Beneloujaephajri, A. Costa, F. L'Haridon, J.P. Métraux, M. Binda, Production of reactive oxygen species and wound-induced resistance in *Arabidopsis thaliana* against *Botrytis cinerea* are preceded and depend on a burst of calcium, BMC Plant Biol. 13 (2013) 160, <http://dx.doi.org/10.1186/1471-2229-13-160>.
- [72] S. Abuqamar, S. Ajeb, A. Sham, M.R. Enan, R. Iratni, A mutation in the expansin-like A2 gene enhances resistance to necrotrophic fungi and hypersensitivity to abiotic stress in *Arabidopsis thaliana*, Mol. Plant Pathol. 14 (2013) 813–827.
- [73] G. Pogorelko, V. Lionetti, O. Fursova, R.M. Sundaram, M. Qi, S.A. Whitham, A.J. Bgdanove, D. Bellincampi, O.A. Zabolina, *Arabidopsis* and *Brachypodium distachyon* transgenic plants expressing *Aspergillus nidulans* acetyltransferases have decreased degree of polysaccharide acetylation and increased resistance to pathogens, Plant Physiol. 162 (2013) 9–23.
- [74] A.J. Lloyd, J. William Allwood, C.L. Winder, W.B. Dunn, J.K. Heald, S.M. Cristescu, A. Sivakumaran, F.J. Harren, J. Mulema, K. Denby, R. Goodacre, A.R. Smith, L.A. Mur, Metabolomic approaches reveal that cell wall modifications play a major role in ethylene-mediated resistance against *Botrytis cinerea*, Plant J. 67 (2011) 852–868.
- [75] Y. Manabe, M. Nafisi, Y. Verhertbruggen, C. Orfila, S. Gille, C. Rautengarten, C. Cherk, S.E. Marcus, S. Somerville, M. Pauly, J.P. Knox, Y. Sakuragi, H.V. Scheller, Loss-of-function mutation of REDUCED WALL ACETYLATION2 in *Arabidopsis* leads to reduced cell wall acetylation and increased resistance to *Botrytis cinerea*, Plant Physiol. 155 (2011) 1068–1078.
- [76] K. Curvers, H. Seifi, G. Mouille, R. de Rycke, B. Asselbergh, A. Van Hecke, D. Vanderschaeghe, H. Höfte, N. Callewaert, F. Van Breusegem, M. Höfte, Abscissic acid deficiency causes changes in cuticle permeability and pectin composition that influence tomato resistance to *Botrytis cinerea*, Plant Physiol. 154 (2010) 847–860.
- [77] S. Ferrari, R. Galletti, D. Pontiggia, C. Manfredini, V. Lionetti, D. Bellincampi, F. Cervone, G. De Lorenzo, Transgenic expression of a fungal endopolygalacturonase increases plant resistance to pathogens and reduces auxin sensitivity, Plant Physiol. 146 (2008) 669–681.
- [78] V. Flors, L. Leyva Mde, B. Vicedo, I. Finiti, M.D. Real, P. García-Agustín, A.B. Bennett, C. González-Bosch, Absence of the endo-beta-1,4-glucanases Cel1 and Cel2 reduces susceptibility to *Botrytis cinerea* in tomato, Plant J. 52 (2007) 1027–1040.
- [79] C. Chassot, C. Nawrath, J.P. Métraux, Cuticular defects lead to full immunity to a major plant pathogen, Plant J. 49 (2007) 972–980.
- [80] R. Hückelhoven, Cell wall-associated mechanisms of disease resistance and susceptibility, Annu. Rev. Phytopathol. 45 (2007) 101–127.
- [81] D. Bellincampi, F. Cervone, V. Lionetti, Plant cell wall dynamics and wall-related susceptibility in plant–pathogen interactions, Front. Plant Sci. 5 (2014) 228, <http://dx.doi.org/10.3389/fpls.2014.00228>.
- [82] T.S. Nühse, Cell wall integrity signaling and innate immunity in plants, Front. Plant Sci. 3 (2012) 280, <http://dx.doi.org/10.3389/fpls.2012.00280>.
- [83] S. Hok, A. Attard, H. Keller, Getting the most from the host: how pathogens force plants to cooperate in disease, Mol. Plant Microbe Interact. 23 (2010) 1253–1259.
- [84] A. Raiola, V. Lionetti, I. Elmaghraby, P. Immerzeel, E.J. Mellerowicz, G. Salvi, F. Cervone, D. Bellincampi, Pectin methylesterase is induced in *Arabidopsis* upon infection and is necessary for a successful colonization by necrotrophic pathogens, Mol. Plant Microbe Interact. 24 (2011) 432–440.
- [85] B.M. Hallberg, G. Henriksson, G. Pettersson, C. Divne, Crystal structure of the flavoprotein domain of the extracellular flavocytochrome cellobiose dehydrogenase, J. Mol. Biol. 315 (2002) 421–434.